Cellulose (2018) 25:619–629
https://doi.org/10.1007/s10570-017-1561-x

ORIGINAL PAPER

# Toward high-performance fibrillated cellulose-based air filter via constructing spider-web-like structure with the aid of TBA during freeze-drying process

**Zhaoqing Lu · Zhiping Su · Shunxi Song · Yongsheng Zhao · Shanshan Ma · Meiyun Zhang**

Received: 25 July 2017 / Accepted: 7 November 2017 / Published online: 10 November 2017


**Abstract** In consideration of the healthcare issues caused by Particulate Matter (PM) pollution, developing high-performance air-filter materials especially aiming at filtering $PM_{2.5}$ has attracted great attention. In this work, we fabricated a novel air filter with spider-web-like structure based on renewable and biodegradable fibrillated cellulose fibers, and demonstrated an effective strategy for network structure regulation during freeze-drying process. The results showed that the air filter with spider-web-like structure, whose filtration efficiency for model PM particles with the diameter of 300 nm could exceed 99%, was obtained from a fibrillated cellulose fiber/water/Tert-Butyl Alcohol (TBA) mixture by freeze-drying. The role of TBA in the construction of spider-web-like structure was mainly due to the following two aspects: (1) TBA molecules could promote the separation of microfibrils which acted as the cobwebs in spider-web-like structure. (2) The presence of TBA resulted in air filter transformed from lamellar porous architecture into spider-web-like structure by changing the morphologies and growth kinetics of ice-crystals. Herein, this work paves a way to fabricate high-performance air filters based on renewable materials and the pore-formation mechanism can provide a guide for structure regulation in porous materials.

**Keywords** Fibrillated cellulose fibers · Tert-butyl alcohol · Spider-web-like structure · Freeze-drying · Air filter

**Electronic supplementary material** The online version of this article (https://doi.org/10.1007/s10570-017-1561-x) contains supplementary material, which is available to authorized users.

Zhaoqing Lu and Zhiping Su have contributed equally to this work.

Z. Lu · Z. Su · S. Song · Y. Zhao (✉) · S. Ma · M. Zhang (✉)
College of Bioresources Chemical and Materials Engineering, Shaanxi Provincial Key Laboratory of Papermaking Technology and Specialty Paper Development, Key Laboratory of Paper Based Functional Materials of China National Light Industry, Shaanxi University of Science and Technology, Xi'an 710021, China
e-mail: zhaoyongsheng@sust.edu.cn; yongshengzhao123@163.com

M. Zhang
e-mail: myzhang@sust.edu.cn

## Introduction

With the rapid development of human community and the boosted urbanization and industrialization, the Particulate Matter (PM) pollution in atmosphere caused by the coal combustion and motor vehicles has caused serious threats to human health (Wang et al. 2014; Yang et al. 2015; Li et al. 2016; Zhang et al. 2016). Especially, particulate matter with diameter smaller than 2.5 μm ($PM_{2.5}$) has a serious impact as it easily penetrates into human lungs and body respiratory system. The

certificated official statistics has shown that $PM_{2.5}$ resulted in high death rate since it could cause coronary blockage, congestive heart-failure, and lung carcinoma (Lee et al. 2015; He et al. 2016; Zhao et al. 2016). Given the health-attack problems, numerous researchers have paid considerable attention to developing air filters with high filtration efficiency for separating $PM_{2.5}$ from polluted air. Nonwoven fabrics are the popular products and generally fabricated from various polymeric nanofibers by electrospining technology (Shi et al. 2013; Zhang et al. 2016). However, the application of these products is limited because of the unrenewable raw materials (Heydarifard et al. 2016), the requirement of chemical agents (Yoon et al. 2016), and the non-biodegradable waste filters (MacFarlane et al. 2012; Heydarifard et al. 2016). Therefore, it is necessary to prepare air filters based on the renewable, sustainable, and biodegradable materials.

Cellulose fiber, a green, renewable and biodegradable polymer, is generally composed of repeating link of 1,4-β-D-glucose and presents excellent biodegradability (Khalil et al. 2014). In this regard, cellulose fiber has been a promising candidate for preparing new generation air filter materials (Mao et al. 2008; MacFarlane et al. 2012; Jahangiri et al. 2014). Plenty of previous reports showed that smooth surface of natural cellulose fibers limited their capture efficiency for PMs (Mao et al. 2008; MacFarlane et al. 2012; Jahangiri et al. 2014), while fibrillated cellulose fibers obtained by mechanical preprocessing exhibited higher capture efficiency for PMs due to the large amount of attached microfibrils (MacFarlane et al. 2012). Thus, the development of air-filter materials based on the fibrillated cellulose fibers has been a hot topic. MacFarlane et al. demonstrated the increased fibrillation degree of cellulose fibers could effectively improve the capture efficiency of prepared air filters (MacFarlane et al. 2012). Mao et al. (2008) prepared an excellent air filter ($\sim$ 95% filtration efficiency) by introducing fibrillated cellulose fibers into the structure of paper-filters. Jahangiri et al. (2014) reported that the addition of fibrillated cellulose fibers into raw materials system can remarkably enhance the filtration efficiency of produced air filters. Howerer, the filtration efficiency of aforementioned cellulosed-based air filters could not reach to 99%, meaning failure to meet the industrial N99 standard (Thiessen 2006).

In order to improve the filtration efficiency of fibrous air filters, many researches have been committed to design air filter materials with various structures such as sandwich structure (Yang et al. 2015), 3D functional structure (Wang et al. 2012; Zhang et al. 2016), and network structure (Oh et al. 2012; Pant et al. 2012; Nemoto et al. 2015). As a matter of fact, fiber diameter and cavity structure play key roles in filtration performance of fibrous air filters (Liu et al. 2015). Hence, great efforts have been made on regulating the fibrous network structures at multiscale by composite combination and special design (Oh et al. 2012; Pant et al. 2012; Nemoto et al. 2015), which are inevitably in favor of expanding the applications of air filters. To achieve this multiscale network structures, the raw fibers must possess two different fiber dimensions and can self-assembly into network structures (Pant et al. 2014). Fibrillated cellulose fiber containing microfibrils and coarse fibers (Wang et al. 2015) has possibility for constructing network-like structure. However, there is still an obstacle to be overcome as these microfibrils are inclined to entangle during conventional drying process (MacFarlane et al. 2012).

Freeze-drying has been demonstrated as an effective technique in fabricating various cellulose-based porous materials including cellulose-based foams (Dash et al. 2012), nanofibrillated cellulose aerogels (Sehaqui et al. 2011), and cellulose-based filter materials (MacFarlane et al. 2012; Yoon et al. 2016). Generally, water and other organic solvents such as methanol, ethanol, pentane and tert-buty alcohol can be used as the freeze-drying medium for preparing porous materials (Yoon et al. 2016). Meanwhile, in comparison with water (Yoon et al. 2016), Tert-butyl alchol (TBA) showed great potential as an ideal freeze-drying medium due to its lower surface tension (Sehaqui et al. 2011), higher vapor pressure, and higher melting point (Ni et al. 2001). TBA also showed great advantages in preparing nanofibrillated cellulose aerogels (Sehaqui et al. 2011), nanocellulose aerogel-containing air filters (Nemoto et al. 2015), and micro-porous cellulose-based filters (Yoon et al. 2016). Hence, TBA give us an opportunity to tune the hydrogen bonding interaction between different cellulose fibers and thus making it possible to regulate the network-like structure of fibrillated cellulose fiber-based porous material during freeze-drying process.

In this study, a mixture of water/TBA was used as medium for freeze-drying process. And we fabricated a

porous material based on fribrillated cellulose fibers and investigated the structure and air filtration performance of this porous material. The content of TBA was varied in order to compare the influence of TBA content on the porous microstructure of final products. Interestingly, it was demonstrated that the addition of TBA could favor an isotropic spider-web-like porous architecture, while the change in TBA content had negligible effect on microstructure. At the same time, after the evaluation of filtration testing aiming at model particles with diameter of 300 nm ($PM_{0.3}$ is the most penetrating particle size, MPPS) (Thiessen 2006), it showed a great potential for taking this spider-web-like porous materials as $PM_{2.5}$ air filters. Its filtration efficiency reached (99.07–99.78%) and even met N99 standard. Our work focused on the formation of spider-web-like structure in fibrillated cellulose fibers-based air filters and the structure regulation mechanisms in TBA/water mixture. We believe this work may offer a meaningful reference for the preparation of high performance air filters through green, renewable, and biodegradable cellulose-based resources.

## Materials and methods

### Materials

The cellulose fiber used in this study was softwood bleached kraft pulp with solid content of 95.3%, which was purchased from Shan Dong Pulp & Paper Co., Ltd. (China). Analytical grade Tert-butyl alcohol (TBA) was used as received from Tianjin Damao Chemical Reagent Plant (China).

### Sample preparation

The preparation procedure of cellulose-based air filters is outlined in Fig. 1. Firstly, cellulose fiber suspension was prepared by disintegrating softwood pulp boards in water using a Lorentzen & Wettre disperser (Sartorius, Germany). Then cellulose fibers were refined by a KRK PFI refiner (Kumagai Riki Kogyo, Japan) to obtain fibrillated cellulose fibers with beating degree of 90 $^{o}$SR. Next, fibrillated cellulose fibers were diluted by pure water or TBA/water mixture to obtain pulp suspension. The concentration of pulp suspension was fixed as 1.5% and the content of TBA was varied. Afterwards, the mixtures were solidified by freezing in a chamber at − 56 °C. Finally, the solidified samples were dried by a BILON freeze-dryer (Shanghai Bilang Instrument Manufacture Co., Ltd, China) at − 56 °C under the pressure of 10 Pa for 72 h. For simplicity, air filters obtained from TBA/water suspension were named as TBA-air filters. At the same time, the control sample was named as C-air filter. The detailed preparation steps were provided in supporting information.

### Characterization

The morphological properties of fibrillated fibers and air filters were observed by a FEI Q45 + EDAX

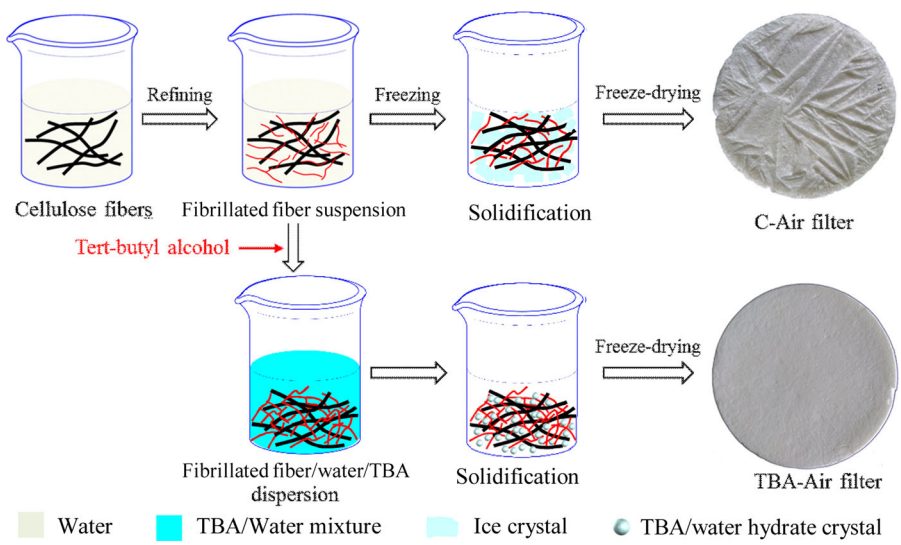


**Fig. 1** Schematic diagram of the preparation procedure of cellulose-based air filters

Octane Prime scanning electron microscopy SEM (FEI, America) at operation voltage of 25 kV. A thin Au layer was sputtered on the samples before observing.

The filtration performance of produced air filters were measured using a LZC-K1 filter testing apparatus (Suzhou Huada Instrument Manufacture Co., Ltd, China), which is consisted of a nebulizer for generating fine particles, a particles counter for determining the consistency of upstream particles ($C_{upstream}$) and downstream particles ($C_{downstream}$), and a filter holder for fixing air filters according to European standard EN 1822-3:2000. For air filters, there is a most penetrating particle size (MPPS) which corresponds to particle diameter of 300 nm ($PM_{0.3}$). The filtration efficiency of air filter for $PM_{0.3}$ is lower than PMs with other size (Thiessen 2006). Therefore, we used simulated particles with diameter of 300 nm for evaluating filtration performance of air filters. The effective measurement area, flow rate though air filter, total measuring time, relative humidity, and temperature corresponded to a value of 100 $cm^2$, 32 L/min, 10 s, room temperature (28 °C), and 40% RH in the test. The particle filtration efficiency ($\eta$) and pressure drop ($\Delta P$) were calculated according to Eqs. (1) and (2).

$$\eta = 1 - \frac{C_{downstream}}{C_{upstream}} \quad (1)$$

$$\Delta P = P_{upstream} - P_{downstream} \quad (2)$$

The specific surface area of air filters was determined from $N_2$ absorption isotherms by performing on a Gemini VII2390 $N_2$ absorption apparatus (Micromeritics, USA). The samples were degassed by $N_2$ blowing at 105 °C for 1 h before measuring.

The air filter samples were compressed in an AI-700-NGD universal material testing apparatus (Taiwan) which was equipped with a load cell of 500 kgf for measuring their dynamic compression properties at room temperature. The compression speed of the load cell was set at 2 mm/min.

## Results and discussion

### The effect of fibrillation treatment on the morphologies of cellulose fibers

Figure 2 shows the microstructures and morphologies of the untreated cellulose fibers and fibrillated cellulose fibers. A dramatic difference in fiber size and morphology is observed. It can be seen from Fig. 2a that original cellulose fibers present smooth surface and uniform size in diameter of $\sim$ 25 μm. As expected, a great number of microfibrils are peeled off from the surface of cellulose fibers due to mechanical exfoliation during refining process as shown in Fig. 2b. This phenomenon is strongly correlated with the intrinsic hierarchical architecture of the nature cellulose fibers (Banavath et al. 2011). Effective exfoliation results in multiscale fiber morphology, i.e., the microfibrils loosely packed around the coarse fibers. This unique structure made it possible for fibrillated cellulose fibers to construct a spider-web-like network by assembly the microfibrils on the frameworks of coarse fibers.

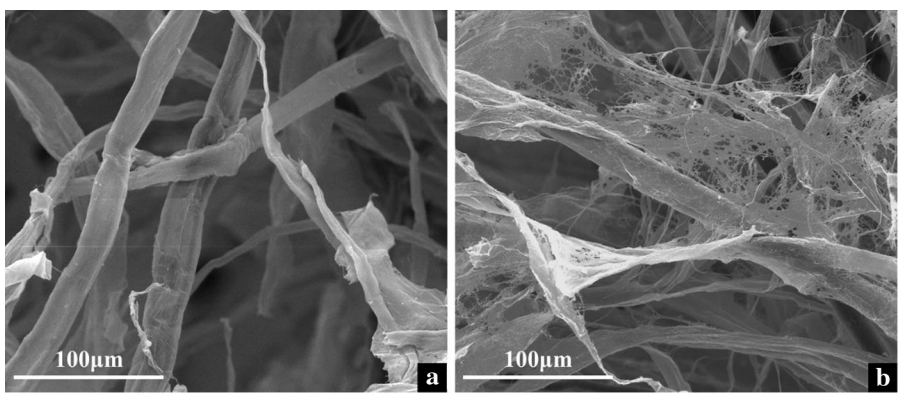


**Fig. 2** Morphological comparison of original fibers (**a**) and fibrillated fibers (**b**)

The effect of TBA addition on the surface morphology of air filters

The surface morphologies of C-air filter and TBA-air filters are shown in Fig. 3a–e. It can be found that the microfibrils are inclined to aggregate and still attached to the surface of coarse fibers before adding TBA. Undesirable interconnection and weak interaction between different cellulose fibers cause a non-uniform pore with broad distribution. In contrast, Fig. 3b–e reveal that microfibrils start to be separated in the form of monofilament after introducing TBA. In addition, spider-web-like structures with smaller and more uniform pore size are observed, which is mainly due to the extensive interconnection between different microfibrils and the resultant framework structures constructed by coarse fibers. Hence, the existence of TBA is favorable for the formation of spider-web-like structures in final air filters, in which TBA promotes the separation of microfibrils. The separation mechanism of microfibrils by TBA is analyzed and presented in Fig. 4. When pure water is used as medium, the intermolecular hydrogen-bonding interaction between different microfibrils can easily occur

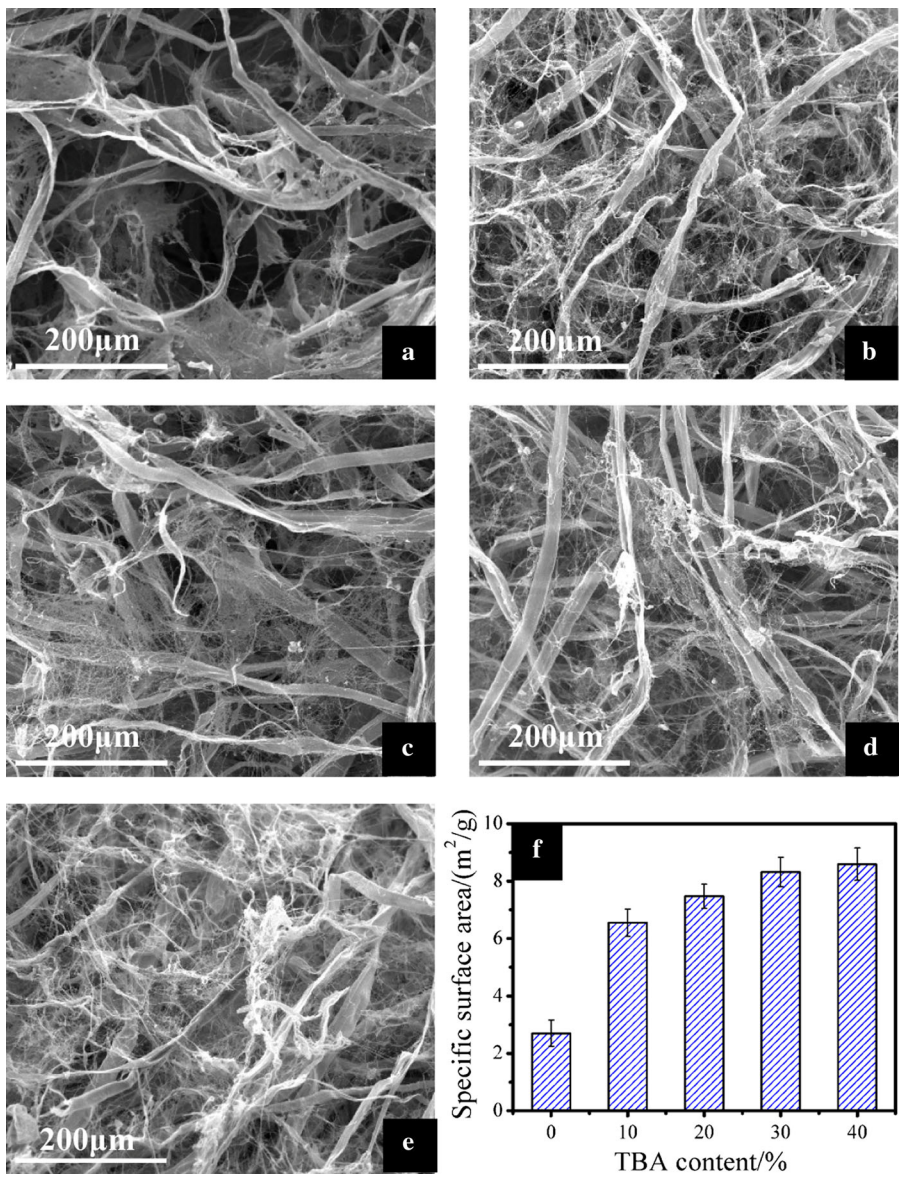


**Fig. 3** **a–e** Surface morphologies of produced air filters with fibrillated cellulose fibers/water/TBA mixture at the TBA content of **a** 0%, **b** 10%, **c** 20%, **d** 30%, **e** 40%, respectively. **f** The relationship between TBA content and specific surface area of produced air filters

due to the numerous free hydroxyls on the surface of microfibrils. In this way, it is difficult to avoid the agglomeration of microfibrils especially when the porous materials are dried. However, TBA molecules can easily attach to the surface of microfibrils through hydrogen-bonding interaction, which leads to hydrophobic surfaces of microfibrils by introducing tert-butyl groups. As a result, the chemical steric hindrance effect of tert-butyl groups can restrict the self-association behaviors of microfibrils (Chem et al. 2012; Jiang and Hsieh 2014). At the same time, the content of TBA can thus be used to easily tune the interfacial interactions between different microfibrils.

In addition, for a quantitative analysis, specific surface area of these filters is shown in Fig. 3f. It is demonstrated that the addition of TBA can improve specific surface area of air filters. When 10–40% TBA are added, specific surface area of air filters can be largely improved by 143–218%. The apparent improvement in specific surface area can also be supported by SEM observations, indicating that after adding TBA, the spider-web-like structures netted by microfibrils with higher specific surface area formed in cellulose-based air filters.

## The effect of TBA addition on the Z-direction morphology

In order to deeply explore the effect of TBA on the formation of this unique spider-web-like structure, the Z-direction morphology of these air filters are compared in Fig. 5a–e. It can be found that Z-direction microstructure of C-air filter presents anisotropic lamellar porous architecture with microfibrils tightly attached on the pore walls. Interestingly, after adding TBA, Z-direction microstructures of produced air filters transformed from anisotropic lamellar porous structure into isotropic spider-web-like porous structure as shown in Fig. 5b–e.

The particular Z-direction microstructure of C-air filter can be mainly attributed to that the lamellar porous structure is strongly dependent on the ice-crystal structure and its growth kinetics. A typical hexagonal ice-crystal with a preferential growth

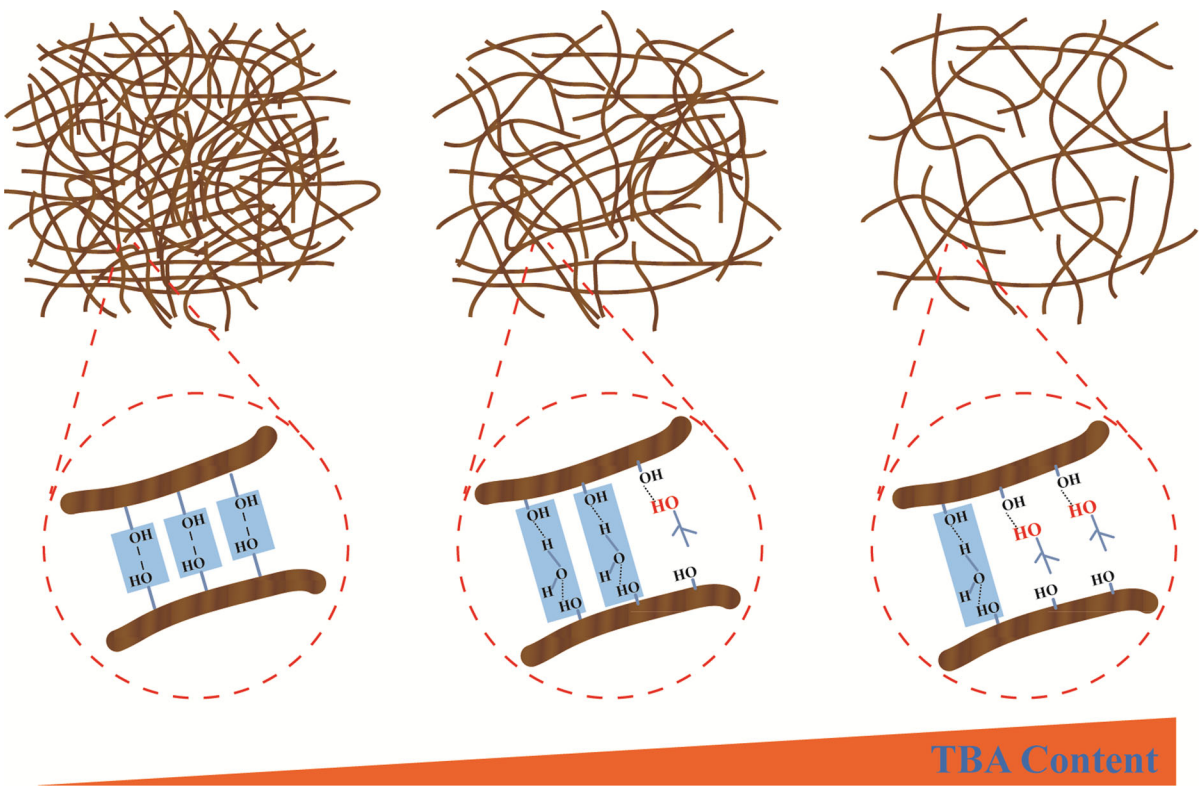


**Fig. 4** A schematic diagram for illustrating the action mechanism of TBA in preventing hydrogen bonding between microfibrils

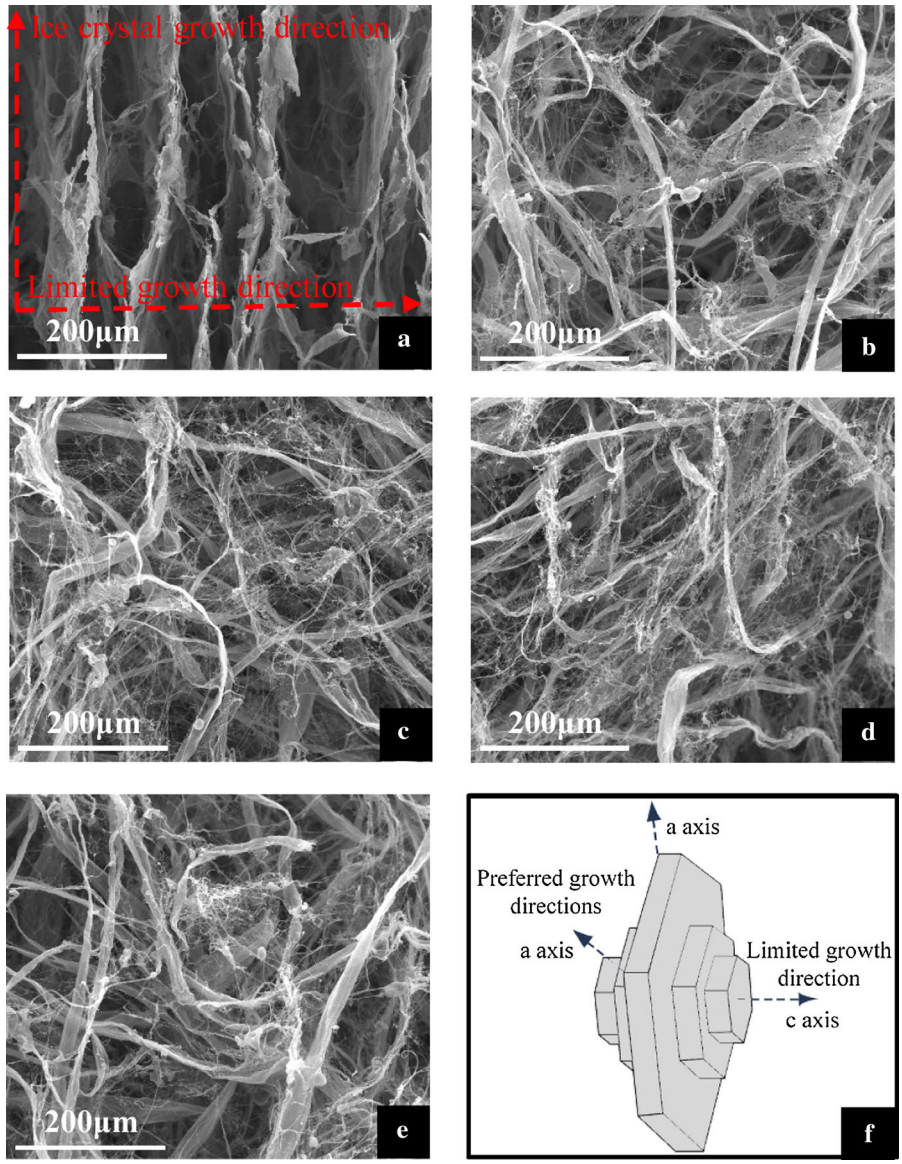


**Fig. 5** **a–e** Z-direction morphologies of produced air filters with fibrillated cellulose fibers/water/TBA mixture at the TBA content of **a** 0%, **b** 10%, **c** 20%, **d** 30%, **e** 40%, respectively. **f** A schematic of crystal structure of ice and anisotropy of ice crystal growth kinetics

direction (a-axis) and a limited growth direction (c-axis) during growth process can be found in Fig. 5f. The velocity of ice front parallel to the crystallographic a-axis is $10^2$–$10^3$ times higher than that parallel to c-axis, thus leading to an ice platelet with large anisotropy (Deville 2008; Hu et al. 2016). It is reported that this platelet-like ice-crystals could reject small size cellulose fibers such as NFC, MFC into the interstitial regions between ice-crystals, resulting in the pore walls with sheet structures (Svagan et al. 2008; Sehaqui et al. 2010). Therefore, the unique lamellar porous structure of C-air filter derived from the strong rejection effect of ice crystals for microfibrils during freezing process. In addition, Nemoto and his coworkers have demonstrated that addition of TBA into the nanocellulose/pure water mixture could induce nanocellulose network with small pores (Nemoto et al. 2015). And the existence of TBA molecules can form small-sized TBA hydrate crystal with a large number of water molecules (Kasraian and DeLuca 1995; Nemoto et al. 2015), making the reject effect from ice-crystals to be ineffective. Thus, the formation of spider-web-like porous structures in TBA-air filters can be ascribed to that TBA can effectively restrict the

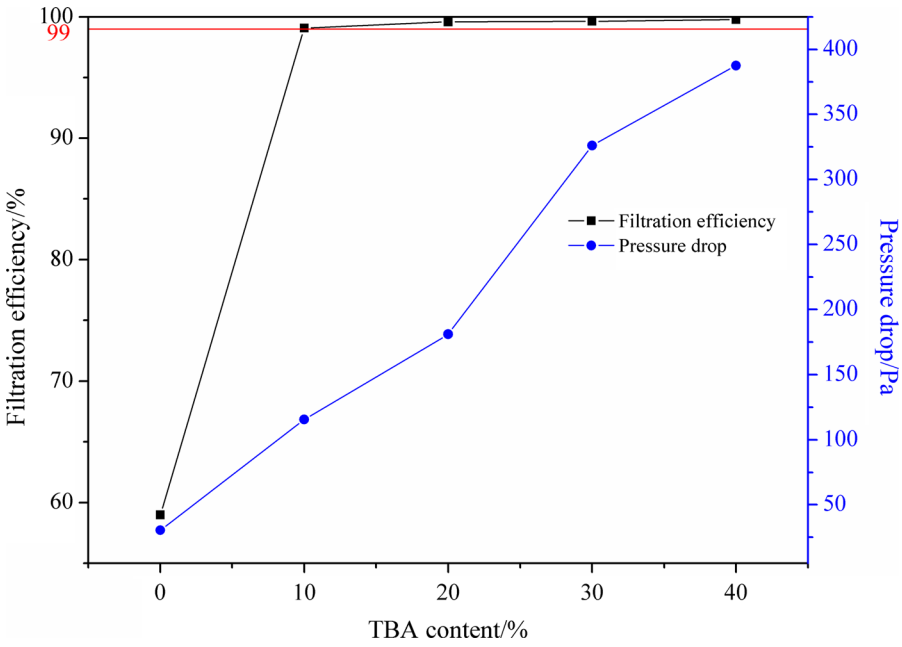


**Fig. 6** Filtration efficiency and pressure drop of produced air filters as a function of TBA content

reject effect of anisotropic ice crystals on the microfibrils.

## The effect of TBA addition on the filtration performance of air filters

The air filtration performance of these air filters for model particles with diameter of 300 nm (MPPS) is shown in Fig. 6. It can be found that air filtration efficiency of prepared air filters can exceed 99% for TBA-air filters with spider-web-like structures. The filtration efficiency even meets the requirement of N99 standard, indicating spider-web-like structures are beneficial for improving filtration efficiency. The improvement in filtration efficiency of TBA-air filters can be assigned to following reasons. One is that increased specific surface area of those well-interconnected microfibrils favors high absorption ability for PMs. The other is that spider-web-like networks with smaller pores can enhance the physical interception capacity for particulate particles (PMs) in comparison with lamellar porous structure. The filtration efficiency ($\eta$) can reflect the capturing capacity for PMs of air filters. Figure 6 shows that $\eta$ increases from $\sim$ 59% to a high level of exceeding 99% after the addition of TBA. This value approaches to the filtration efficiency (99.99%) of petroleum-based high-performance air filters (Yang et al. 2015; Zhang et al. 2016, 2017a, b), indicating TBA-air filters hold great competitiveness in air filtration field. In addition, pressure drop ($\Delta P$), a highly effective parameter to reflect airflow resistance and the existence of defects in the networks, exhibits a sharp increase when adding TBA, meaning the formation of impeccable spider-web-like structures. And a further increase of $\Delta P$ is achieved with the increase of TBA content, which means that the coverage rate of this special spider-web-like structure was gradually improved. Hence, the filtration performance of TBA-air filters is greatly dependent on the completeness of spider-web-like networks.

## Dynamic compression performance of air filters

In addition, mechanical properties especially the compression performance is a key issue for these air filters under working conditions. The dynamic compression stress–strain curves of C-air filter and TBA-air filters are shown in Fig. 7. It can be found that the curves exhibit a typical shape with two regions including linear-modulus zone and strain-hardening zone. The modulus is related with the strength of fibers and interfacial interactions between different fibers. It is indicated that the compression modulus gradually

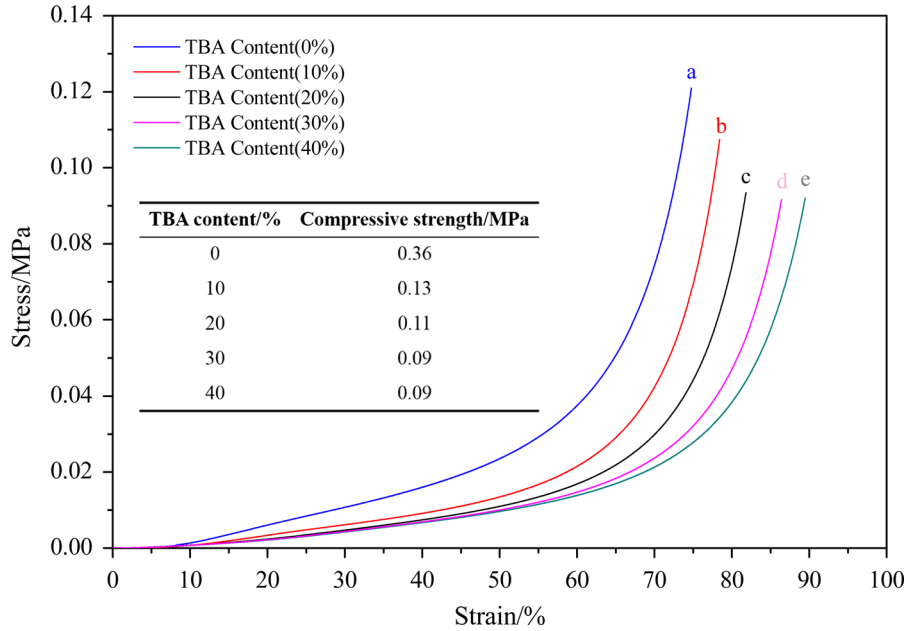


| TBA content/% | Compressive strength/MPa |
|---|---|
| 0 | 0.36 |
| 10 | 0.13 |
| 20 | 0.11 |
| 30 | 0.09 |
| 40 | 0.09 |

**Fig. 7** Dynamic compression stress–strain curves of produced air filters at different TBA content. The inserted table lists the compressive strength of these air filters

decrease with the increase in TBA content since TBA can weaken the intermolecular hydrogen-bonding interaction between adjacent microfibrils (Korehei et al. 2016). At the strain hardening region, a further increase of mechanical strength reflects the enhanced resistance of pore fracture. Furthermore, the inserted table in Fig. 7 shows that the final compression strength decreases when adding TBA. This is consistent with the fact that the introduction of TBA can lead to Z-direction microstructures of air filters transform from lamellar porous structure into spider-web-like structure (Fig. 5). Because the presence of bridging-link in lamellar porous structure can prevent Euler buckling of lamellar pore walls and contribute to higher compression strength (Deville et al. 2006). Overall, the compression strength of TBA-air filters makes is suitable for being used as mechanical reliable air filters.

## Conclusions

In summary, we developed an effective and environment-friendly method to prepare high-performance air filters by freeze-drying process. The addition of TBA into the aqueous fibrillated cellulose fiber suspension induced a structure transformation from lamellar porous architecture into the unique spider-web-like structure, which greatly increased the specific surface area of TBA-air filters by 143–218% in comparison with that of the control sample (C-air filter). The effect of TBA on the formation of this unique spider-web-like structure is mainly summarized into two mechanisms. One is that TBA molecules are inclined to separate the microfibrils by weakening the intermolecular hydrogen-bonding interaction. The other is that the crystal structure and growth kinetics of ice-crystals, which plays a key role in the pore formation of cellulose-based porous materials during freeze-drying process, were remarkably altered by TBA molecules. In addition, these TBA-air filters possess excellent capturing capacity for model PMs with diameter of 300 nm. The air filtration efficiency of these TBA-air filters can even reach a high level of 99.07–99.78%.

**Acknowledgments** The authors would like to acknowledge the financial support from National Science Foundation of China (Grant No. 31670593), State Key Laboratory of Pulp and Paper Engineering (201601), State Key Laboratory for modification of chemical fibers and polymer materials (LK1601), Shaanxi Province as a Whole the Innovation Project of Science and Technology Plan Projects (2016KTCQ01-87), Education Department of Shaanxi

Provincial Government (15JF012), and Science and Technology Department of Shaanxi Province (2015KJXX-34). We appreciate Suzhou Huada Instrument and Equipment LTD. very much for friendly providing tests for us.

## References

Banavath HN, Bhardwaj NK, Ray AK (2011) A comparative study of the effect of refining on charge of various pulps. Bioresour Technol 102:4544–4551

Chem JM, Chun S, Choi E et al (2012) Eco-friendly cellulose nanofiber paper-derived separator membranes featuring tunable nanoporous network channels for lithium-ion batteries. J Mater Chem 22:16618–16626

Dash R, Li Y, Ragauskas AJ (2012) Cellulose nanowhisker foams by freeze casting. Carbohydr Polym 88:789–792

Deville S (2008) Freeze-casting of porous ceramics: a review of current achievements and issues. Adv Eng Mater 10:155–169

Deville S, Saiz E, Nalla RK, Tomsia AP (2006) Freezing as a path to build complex composites. Science 311:515–518

He M, Ichinose T, Kobayashi M et al (2016) Differences in allergic inflammatory responses between urban PM2.5 and fine particle derived from desert-dust in murine lungs. Toxicol Appl Pharmacol 297:41–55

Heydarifard S, Nazhad MM, Xiao H, Shipin O (2016) Water-resistant cellulosic filter for aerosol entrapment and water purification, part I: production of water-resistant cellulosic filter. Environ Technol 37:1716–1722

Hu X, Yang L, Li L et al (2016) Freeze casting of composite system with stable fiber network and movable particles. J Eur Ceram Soc 36:4147–4153

Jahangiri P, Madani A, Korehei R et al (2014) On filtration and heat insulation properties of foam formed cellulose based materials. Nord Pulp Pap 29:584–591

Jiang F, Hsieh Y (2014) Assembling and redispersibility of rice straw nanocellulose: effect of tert-butanol. ACS Appl Mater Interfaces 6:20075–20084

Kasraian K, DeLuca PP (1995) Thermal analysis of the tertiary butyl alcohol–water system and its implications on freeze-drying. Pharm Res 12:484–490

Khalil HPSA, Davoudpour Y, Islam N et al (2014) Production and modification of nanofibrillated cellulose using various mechanical processes: a review. Carbohydr Polym 99:649–665

Korehei R, Jahangiri P, Nikbakht A et al (2016) Effects of drying strategies and microfibrillated cellulose fiber content on the properties of foam-formed paper. J Wood Chem Technol 36:235–249

Lee CJ, Martin RV, Henze DK et al (2015) Response of global particulate-matter-related mortality to changes in local precursor emissions. Environ Sci Technol 49:4335–4344

Li S, Williams G, Guo Y (2016) Health benefits from improved outdoor air quality and intervention in China. Environ Pollut 214:17–25

Liu B, Zhang S, Wang X et al (2015) Efficient and reusable polyamide-56 nanofiber/nets membrane with bimodal structures for air filtration. J Colloid Interface Sci 457:203–211

MacFarlane AL, Kadla JF, Kerekes RJ (2012) High performance air filters produced from freeze-dried fibrillated wood pulp: fiber network compression due to the freezing process. Ind Eng Chem Res 51:10702–10711

Mao J, Grgic B, Finlay WH et al (2008) Wood pulp based filters for removal of sub-micrometer aerosol particles. Nord Pulp Pap 23:420–425

Nemoto J, Saito T, Isogai A (2015) Simple freeze-drying procedure for producing nanocellulose aerogel-containing, high-performance air filters. ACS Appl Mater Interfaces 7:19809–19815

Ni N, Tesconi M, Tabibi SE et al (2001) Use of pure t-butanol as a solvent for freeze-drying: a case study. Int J Pharm 226:39–46

Oh HJ, Pant HR, Kang YS et al (2012) Synthesis and characterization of spider-web-like electrospun mats of meta-aramid. Polym Int 61:1675–1682

Pant HR, Park CH, Tijing LD et al (2012) Bimodal fiber diameter distributed graphene oxide/nylon-6 composite nanofibrous mats via electrospinning. Colloids Surf A Physicochem Eng Asp 407:121–125

Pant HR, Kim HJ, Joshi MK et al (2014) One-step fabrication of multifunctional composite polyurethane spider-web-like nanofibrous membrane for water purification. J Hazard Mater 264:25–33

Sehaqui H, Salajková M, Zhou Q, Berglund LA (2010) Mechanical performance tailoring of tough ultra-high porosity foams prepared from cellulose I nanofiber suspensions. Soft Matter 6:1824–1832

Sehaqui H, Zhou Q, Berglund LA (2011) High-porosity aerogels of high specific surface area prepared from nanofibrillated cellulose (NFC). Compos Sci Technol 71:1593–1599

Shi L, Zhuang X, Tao X et al (2013) Solution blowing nylon 6 nanofiber mats for air filtration. Fibers Polym 14:1485–1490

Svagan AJ, Samir MASA, Berglund LA (2008) Biomimetic foams of high mechanical performance based on nanostructured cell walls reinforced by native cellulose nanofibrils. Adv Mater 20:1263–1269

Thiessen RJ (2006) Filtration of respired gases: theoretical aspects. Respir Care Clin N Am 12:183–201

Wang N, Wang X, Ding B et al (2012) Tunable fabrication of three-dimensional polyamide-66 nano-fiber/nets for high efficiency fine particulate filtration. J Mater Chem 22:1445–1452

Wang N, Zhu Z, Sheng J et al (2014) Superamphiphobic nanofibrous membranes for effective filtration of fine particles. J Colloid Interface Sci 428:41–48

Wang S, Peng X, Zhong L et al (2015) An ultralight, elastic, cost-effective, and highly recyclable superabsorbent from microfibrillated cellulose fibers for oil spillage cleanup. J Mater Chem A 3:8772–8781

Yang Y, Zhang S, Zhao X et al (2015) Sandwich structured polyamide-6/polyacrylonitrile nanonets/bead-on- string composite membrane for effective air filtration. Sep Purif Technol 152:14–22

Yoon Y, Kim S, Ahn KH, Ko KB (2016) Fabrication and characterization of micro-porous cellulose filters for indoor air quality control. Environ Technol 37:703–712

Zhang S, Tang N, Cao L et al (2016) Highly integrated polysulfone/polyacrylonitrile/polyamide-6 air filter for

multilevel physical sieving airborne particles. ACS Appl Mater Interfaces 8:29062–29072

Zhang S, Liu H, Yin X et al (2017a) Tailoring mechanically robust poly(m-phenylene isophthalamide) nanofiber/nets for ultrathin high-efficiency air filter. Sci Rep 7:40550–40561

Zhang S, Liu H, Zuo F et al (2017b) A controlled design of ripple-like polyamide-6 nanofiber/nets membrane for high-efficiency air filter. Small 13:1603151–1603161

Zhao X, Wang S, Yin X et al (2016) Slip-effect functional air filter for efficient purification of PM2.5. Sci Rep 6:35472–35483